Catalysis Communications 88 (2017) 22–25

Contents lists available at ScienceDirect

Catalysis Communications

journal homepage: www.elsevier.com/locate/catcom

Short communication

Constructing $BiO_{1.1}Br_{0.8}$ sheet-sphere junction structure for efficient photocatalytic degradation of aniline

Yuan Guan [a,b], Shaomang Wang [b,c,*], Yu Liu [b], Lei Lu [c], Yan Huang [b], Yongbo Wang [b], Xin Wang [a]

[a] Key Laboratory for Soft Chemistry and Functional Materials of Ministry Education, Nanjing University of Science and Technology, Nanjing 210094, PR China
[b] School of Environment and Safety Engineering, School of Huai De, Changzhou University, Changzhou 213164, PR China
[c] Eco-Materials and Renewable Energy Research Center (ERERC), College of Engineering and Applied Sciences, Nanjing University, Nanjing 210093, China

ARTICLE INFO

Article history:
Received 23 March 2016
Received in revised form 9 June 2016
Accepted 26 June 2016
Available online 27 June 2016

Keywords:
Sheet-sphere junction
$BiO_{1.1}Br_{0.8}$
Photocatalysis
Degradation
Aniline

ABSTRACT

A sheet-sphere junction structure photocatalyst, $BiO_{1.1}Br_{0.8}$ was successfully synthesized by calcining BiOBr at 500 °C for 7 h. The $BiO_{1.1}Br_{0.8}$ exhibited apparently enhanced photocatalytic activity in comparison with BiOBr. About 90% of aniline (50 mL, 50 mg L^{-1}) was degraded over $BiO_{1.1}Br_{0.8}$ (1 g L^{-1}) after LED light irradiation for 4 h. Photocurrent and photoluminescence spectra analyses demonstrated that separation efficiency of photogenerated electron-hole pairs in $BiO_{1.1}Br_{0.8}$ was much higher than that in BiOBr, which greatly improved its photocatalytic activity. The increased pore size of $BiO_{1.1}Br_{0.8}$ was beneficial for projecting light into pore, which promoted the photocatalytic degradation of aniline.

1. Introduction

Over the past decades, photocatalytic technology has attracted great attention because of its potential application in new energy development and pollutants removal [1–6]. Up to date, exploitation of high-performance photocatalytic materials meeting the requirements of practical production is still a huge challenge.

Recently, increasing interest has been focused on BiOBr due to its good photocatalytic activity [7–11]. Currently, the morphologies of BiOBr synthesized are mainly microsphere [12–15] and nanosheet [16,17]. The specific surface area and pore diameter of sphere-like BiOBr are relatively large, which facilitates to adsorb more targets resulting in high photocatalytic activity [18,19]. BiOBr Nanosheet with exposed {001} or {102} or {111} facets is beneficial for the separation of photogenerated electron-hole pairs, which improves its photocatalytic activity [20–24]. In addition, it is noteworthy that some non-stoichiometric BiOBr with Br-vacancies such as Bi_3O_4Br [25], $Bi_{24}O_{31}Br_{10}$ [26], $Bi_{12}O_{17}Br_2$ [27], Bi_5O_7Br [28] and $Bi_4O_5Br_2$ [29] can obviously inhibit the recombination of photoinduced charges, and thereby greatly boost their photocatalytic properties.

Herein, for the first time we construct a sheet-sphere junction structure $BiO_{1.1}Br_{0.8}$ via a facile solvothermal approach coupled with thermal decomposition. The photocatalytic activity of $BiO_{1.1}Br_{0.8}$ is evaluated by decomposing aniline under energy-efficient white LED light irradiation. The mechanisms of apparently enhanced photocatalytic activity will be investigated in detail.

2. Experimental section

2.1. Preparation of $BiO_{1.1}Br_{0.8}$ sheet-sphere junction

BiOBr was prepared through a facile solvothermal method. Typically, 4.9 g of $Bi(NO_3)_3 \cdot 5H_2O$ was dissolved in 40 mL of glycol, which was drop-wisely added into the same volume of glycol containing NaBr (1.0 g). The mixed solution was transferred into an autoclave (100 mL) and reacted at 160 °C for 12 h, after it was vigorously stirred at room temperature for 1 h. The autoclave was naturally cooled to room temperature. The resulting product was washed by deionized water and then dried at 80 °C to obtain BiOBr. The $BiO_{1.1}Br_{0.8}$ sample was synthesized by calcining the as-prepared BiOBr. In a typical experiment, 3.0 g of the as-fabricated BiOBr was placed into a combustion boat, which was heated to 500 °C at a rate of 10 °C min^{-1} in a program-controlled tubular furnace, and then calcined at this temperature for 7 h. After the furnace was naturally cooled to room temperature, the product was taken out and weighted. The $BiO_{1.1}I_{0.8}$ was obtained according to the Eq. (1).

$$BiOBr + \frac{(x-1)}{2}O_2 = BiO_xBr_{3-2x} + (x-1)Br_2 \quad (1)$$

* Corresponding author at: School of Environment and Safety Engineering, School of Huai De, Changzhou University, Changzhou 213164, PR China.
E-mail addresses: gywsm@cczu.edu.cn (S. Wang), wangx@njust.edu.cn (X. Wang).

http://dx.doi.org/10.1016/j.catcom.2016.06.024
1566-7367/

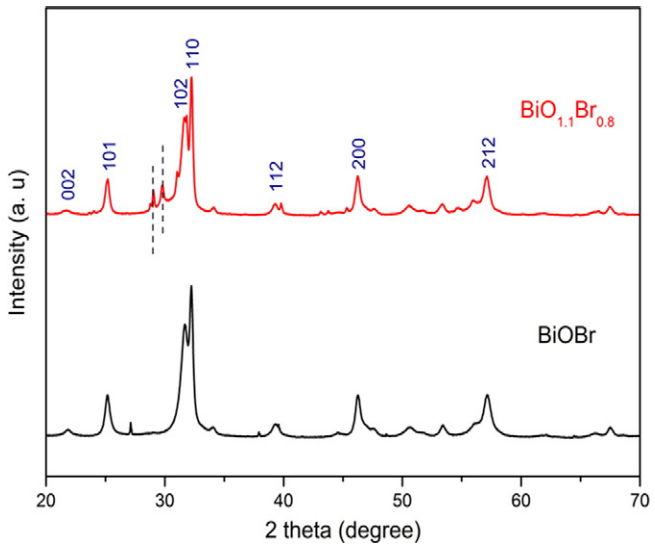

Fig. 1. XRD patterns of BiOBr and $BiO_{1.1}Br_{0.8}$.

2.2. Photocatalytic reaction

The photocatalytic activities of the as-prepared samples were investigated by the degradation of aniline under four groups of white LED lamp board (18 W/lamp board) irradiation. The white LED light consists of three colors of blue, green and red. The main wavelength range of the LED lamp is from 420 nm to 780 nm. In each experiment, 0.05 g of sample was added into 50 mL of aniline solution (50 mg L^{-1}). Prior to irradiation, the suspension was magnetically stirred in the dark for 1 h to reach adsorption–desorption equilibrium between the photocatalyst and aniline solution. At given time intervals, about 5 mL of suspension was taken out, centrifuged and analyzed by a UV–vis spectrophotometer at 280 nm.

3. Results and discussion

3.1. Characterization of the as-prepared samples

The XRD patterns in Fig. 1 display that the diffraction peaks of BiOBr were in good consistent with its tetragonal phase (JCPDS 09-0393). Compared to BiOBr, the primary characteristic peaks of $BiO_{1.1}Br_{0.8}$ didn't obviously change, which indicates that the crystal structure of $BiO_{1.1}Br_{0.8}$ is same as that of BiOBr. In addition, two new peaks locating at about 28.9° and 29.7° were observed in $BiO_{1.1}Br_{0.8}$, which is mainly ascribed to its better crystal form after the calcination of high temperature.

TG measurement was performed to investigate the loss of bromine in BiOBr during thermal treatment. As displayed in Fig. S1, the initial decomposition temperature of BiOBr was about 220 °C. When the calcination temperature was greater than 500 °C, the loss of bromine became apparently. When the calcination temperature was 500 °C, bromine lost very slow. This preliminary indicates that bromine don't completely lose after the calcination of BiOBr.

The morphologies of BiOBr and $BiO_{1.1}Br_{0.8}$ are depicted in Fig. 2. BiOBr was a microsphere-like shape with a diameter of 3–10 μm (Fig. 2a, Fig. S2a and b). The $BiO_{1.1}Br_{0.8}$ presented two different morphologies of microsphere and sheet. The particle diameter of $BiO_{1.1}Br_{0.8}$ microspheres was around 1–8 μm, and the thickness of $BiO_{1.1}Br_{0.8}$ sheets was about 150 nm. The microspheres were connected with the sheets forming a sheet-sphere junction structure (Fig. 2b, Fig. S2c and d). In addition, EDS analyses show that the elements of the sheet structure contained Bi, O and Br, which was the same as those of the microsphere structure (Fig. S2e, f and g). The results of EDS confirm that the sheet is $BiO_{1.1}Br_{0.8}$.

The surface chemical compositions and states of the elements in BiOBr and $BiO_{1.1}Br_{0.8}$ were analyzed by XPS. In Fig. S3a, the peaks of Bi 4f, O 1s and Br 3d identified in BiOBr are in line with its chemical compositions. The peaks of Br 3d observed in $BiO_{1.1}Br_{0.8}$ confirm that Br atoms don't completely lose after the calcination of BiOBr. The peaks of Bi 4f correspond to Bi^{3+} (Fig. S3b), and the peaks of Br 3d fitted into Br $3d_{3/2}$ and Br $3d_{5/2}$ are assigned with Br^- in BiOBr and $BiO_{1.1}Br_{0.8}$ (Fig. S3d) [30].

For BiOBr, the peaks of O 1s could be fitted into two peaks. The first peak at 529.8 eV belongs to crystal O atoms (O^{2-}). Another peak at 531.3 eV originates from O atoms (O^{2-}) of H_2O adsorbing on its surface (Fig. S3c) [31], which disappeared in $BiO_{1.1}Br_{0.8}$ due to high temperature of calcination. In addition, the binding energies of Bi 4f, O 1s and Br 3d in $BiO_{1.1}Br_{0.8}$ shifted to a higher energy in comparison with those in BiOBr. It is due to the fact that the smaller particles of $BiO_{1.1}Br_{0.8}$ enhances the electrostatic attraction between Bi^{3+} and O^{2-} (or Br^-).

3.2. Photocatalytic performance test

Fig. 3 reveals the photocatalytic activities of BiOBr and $BiO_{1.1}Br_{0.8}$ evaluated by degrading aniline under LED light irradiation. The absorbance of aniline solution remained nearly unchanged without photocatalyst under light irradiation for 4 h, indicating that aniline is stable and difficult to be photolysis. After 4 h of light irradiation, about 41% of aniline was decomposed over BiOBr, whereas around 90% of aniline was degraded over $BiO_{1.1}Br_{0.8}$. The degradation rate of aniline over $BiO_{1.1}Br_{0.8}$ was 2.1 times as much as that achieved by BiOBr under the same reaction conditions.

To investigate the time of adsorption equilibrium and the effect of adsorption on photocatalytic degradation, aniline adsorption experiments were carried out over BiOBr and $BiO_{1.1}Br_{0.8}$, respectively. From Fig. S4, aniline adsorption over BiOBr and $BiO_{1.1}Br_{0.8}$ reached

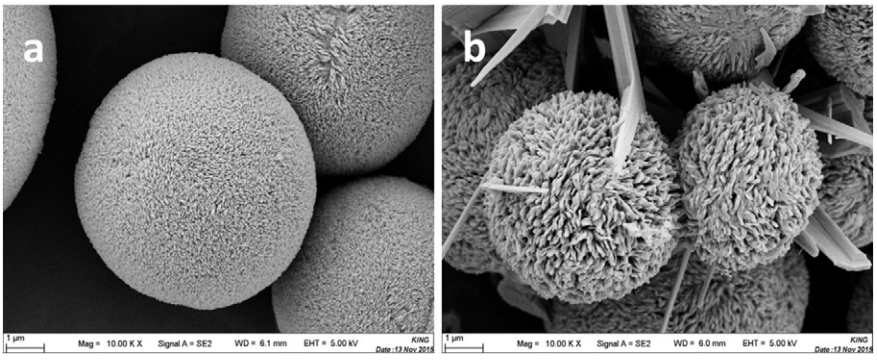

Fig. 2. SEM images of (a) BiOBr and (b) $BiO_{1.1}Br_{0.8}$.